JOURNAL OF GEOPHYSICAL RESEARCH, VOL. 104, NO. D17, PAGES 21,247–21,262, SEPTEMBER 20, 1999

In situ measurements of C_2-C_{10} volatile organic compounds above a Sierra Nevada ponderosa pine plantation

Mark S. Lamanna and Allen H. Goldstein

Division of Ecosystem Sciences, Department of Environmental Science, Policy, and Management, University of California, Berkeley

Abstract. A fully automated gas chromatograph-flame ionization detector system was designed and built to measure ambient concentrations of C_2-C_{10} volatile organic compounds, including many oxygenated compounds, without using liquid cryogen. It was deployed at Blodgett Forest Research Station in Georgetown, California, 38°53'42.9"N, 120°37'57.9"W, 1315 m elevation. More than 900 in situ measurements were made above a ponderosa pine canopy at 40-min intervals, continuously from July 2 through August 1, 1997. Factor analysis and observed temporal patterns were used to categorize sources for measured compounds as biogenic or anthropogenic or both. Compounds that were clearly biogenic included methylbutenol, isoprene and its oxidation products (methacrolein and methyl vinyl ketone), and terpenes (α-pinene, 3-carene, d-limonene). Other compounds were partially biogenic, including acetone, ethene, propene, hexanal, acetaldehyde, and methanol. Hydroxyl radical (OH) loss rates were dominated by the clearly biogenic compounds, accounting for 70% of the loss under mean midday conditions. The most important single compounds were isoprene (33%) and methylbutenol (21%). These two compounds were dominant under all conditions, including the coldest and most polluted days. Under the most polluted conditions, acetaldehyde became very important, accounting for 13% of the total. Total OH loss rates were highly correlated with temperature because emissions of biogenic compounds, which dominate OH loss, are strongly temperature dependent. Much of the research on biogenic volatile organic compounds has focused on isoprene and terpenes. Our results suggest that quantifying and understanding factors controlling biogenic emissions of other compounds such as methylbutenol, acetone, hexanal, methanol, and acetaldehyde are critical for improving our understanding of regional photochemistry.

1. Introduction

Volatile organic compounds (VOCs) from both biogenic and anthropogenic sources are important in tropospheric chemistry as they can influence the oxidative potential of the lower troposphere [e.g., *Trainer et al.*, 1987], contribute to regional and global aerosol budgets via gas-to-particle conversions [e.g. *Zhang et al.*, 1992; *Andreae and Crutzen*, 1997], and are precursors to the formation of tropospheric ozone [*Chameides*, 1988; *National Research Council (NRC)*, 1991]. VOCs define the complete set of volatile organic compounds, while oxygenated volatile organic compounds (OVOCs, those VOCs containing oxygen) and nonmethane hydrocarbons (NMHCs, those VOCs containing only carbon and hydrogen) are subsets of VOCs. While many measurement series have been made for C_2- C_6 NMHCs, the inventory is as yet spatially and temporally inadequate for many biogenic compounds and is extremely limited in the number of studies on OVOCs. A few recent measurements have shown OVOCs to be extremely important. Ambient concentration measurements of 2-methyl-3-butene-2-ol (methylbutenol or MBO) in a remote conifer forest site suggest its impact on regional tropospheric chemistry is on a par with isoprene [*Goldan et al.*, 1993]. Photolysis of acetone may be responsible for up to 50% of the observed peroxyacetyl nitrate (PAN) (a stable and readily transported organic nitrate), as well as being an important source of HO_x radicals in the upper troposphere [*Singh et al.*, 1995]. In addition, VOC field measurements may provide insight into photochemical aging and transport phenomena [*Parrish et al.*, 1992; *McKeen and Liu*, 1993] and plant physiology via biogenic source controls over individual compounds [*Lerdau et al.*, 1997] and could provide a test of laboratory-derived reaction mechanisms [*Montzka et al.*, 1995; *Rudich et al.*, 1995; *Aschmann et al.*, 1996; *Williams et al.*, 1997].

In the four decades since the first investigators identified VOCs and nitrogen oxides (NO_x = NO + NO_2) as the essential precursors in photochemical smog formation, the overall importance of VOCs in planetary boundary layer (PBL) photochemistry has been well established. Studies of urban air shed transport phenomena show that photochemical smog formation is often a regional issue [*NRC*, 1991]. Tropospheric ozone formation is affected by both biogenic and anthropogenic VOCs. Many modeling and field studies have addressed their relative importance [*Trainer et al.*, 1987; *Goldan et al.*, 1995; *Hirsch et al.*, 1996; *Goldstein et al.*, 1998].

The majority of VOC field measurements have focused on an apparently incomplete subset of compounds, including mainly the NMHCs. This narrow focus results from a variety of factors, including the inability to accurately collect and

Paper number 1999JD900289.
0148-0227/99/1999JD900289$09.00

analyze OVOCs, as well as the difficulty in obtaining, creating, and storing OVOC calibration standards.

For this study we designed and built a new instrument for automated in situ measurements of a wide range of VOCs and deployed it in a conifer forest ecosystem in the Sierra Nevada foothills ~75 km east of Sacramento, California. Our goals were to obtain continuous ambient concentration measurements of NHMCs and OVOCs, to apportion the sources of these compounds as either anthropogenic or biogenic or both, and to determine the relative importance of biogenic and anthropogenic VOCs for photochemistry in this region of California. This instrument was designed to be easily configured for three different sample collection schemes: relaxed eddy accumulation (REA) flux, gradient flux, or ambient concentration measurements. In addition, our instrument operates without the use of liquid nitrogen, thus extending the physical range of sites where continuous measurements can be obtained.

2. Methodology

2.1. Measurement Site

VOC measurements were made continuously above a ponderosa pine plantation at 40 min intervals, from July 2 through August 1, 1997. These measurements were part of a larger field experiment at Blodgett Forest Research Station (Georgetown, California, 38°53'42.9"N, 120°37'57.9"W, 1315 m elevation) in the Sierra Nevada foothills to study biosphere-atmosphere exchange of trace gases and energy.

For this experiment we established an automated environmental measurement station monitoring a full suite of chemical and meteorological parameters, including wind speed and direction, net radiation, photosynthetically active radiation (PAR), atmospheric relative humidity, air temperature, soil heat flux, soil temperature, soil moisture, needle temperature, concentrations and fluxes of CO_2, H_2O, and O_3, and fluxes of sensible heat and momentum from June 1 until September 9, 1997. The Sierra Nevada receives the majority of its precipitation between September and May, and little or no rain during the summer. The predominant daytime air mass trajectory at the site was upslope from the Sacramento valley which lies to the west. At night the site received downslope flow from the Sierra Nevada mountains to the east (Figure 1). The soil was in the Cohasset series, a fine-loamy mixed mesic haploxeralf. Ponderosa pines, at this site, break bud in early May and set bud in late July to early August. The plantation was even-aged (5-6 years) and of even height (3-4 m). The open canopy also included a few individuals of douglas fir (*Pseudotsuga menziesii*), white fir (*Abies concolor*), black oak (*Quercus kellogii*), incense cedar (*Calocedrus decurrens*), and sugar pine (*Pinus lambertiana*). Major understory shrubs included manzanita (*Arctostaphylos spp.*) and whitethorn (*Ceonothus cordulatus*). About 55% of the ground area was covered by shrubs, 30% by conifer trees, 2% by deciduous trees, 7% by forbs, 3% by grass and 3% by stumps. (Biomass data courtesy of A. Guenther, National Center for Atmospheric Research (NCAR) (personal communication, 1997)).

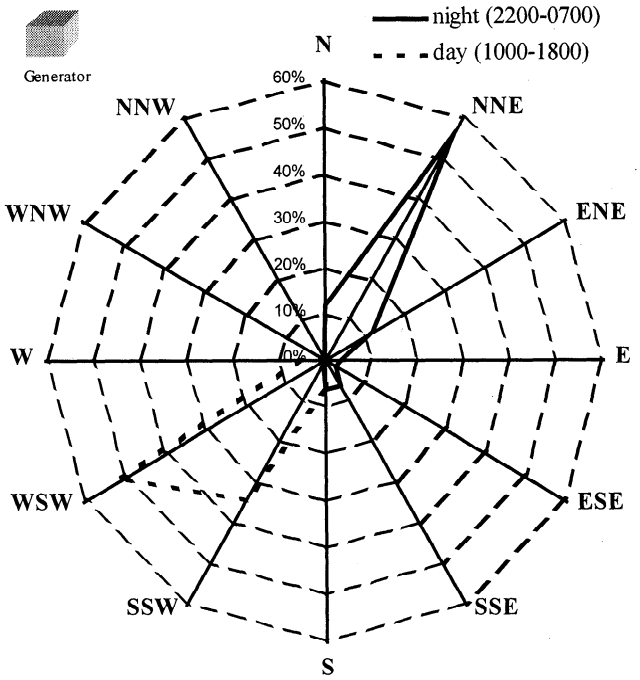

Figure 1. Predominant day time and night time air mass trajectories from the tower site.

2.2. VOC Measurement System

2.2.1. Components of the VOC sampling system. Capillary gas chromatography is the most common method for analyzing VOCs in ambient air samples. A typical gas chromatography (GC) system consists of components that provide for sample collection, enrichment, separation, identification, and quantification. The suite of target compounds to be measured determines system component selection for instrumentation development. We designed and built an instrument to measure ambient concentrations of VOCs (including OVOCs) containing from 2 to 10 carbon atoms, specifically focusing on MBO, isoprene and its oxidation products methyl vinyl ketone (MVK) and methacrolein (MACR), acetone, acetaldehyde, and terpenes, in situ, without the use of liquid cryogen.

2.2.2. Sample flow paths. The measurement system consists of two independent measurement channels. For simplicity, the components of only one channel are depicted in "sampling mode" in Figure 2. The main sample intake was mounted on a walk-up tower (Upright Towers, Selma, California) ~6 m above the forest canopy (9 m above ground level). Ambient air was drawn at 8 L min^{-1} STP through 2 μm Teflon particulate filters (Gelman Sciences, Ann Arbor, Michigan) and 10 m of 3/8 inch OD, 1/4 inch ID Teflon tubing (Chemfluor-Norton Performance Plastics, Wayne, New Jersey) into the instrument shed at ground level, where flow was monitored (MKS Instruments, Andover, Massachusetts). Inlet filters were changed every 10 days. A subsample for analysis was drawn from the center of the main sample tube at 20 cm^3 min^{-1} STP through 0.030 inch ID fused silica lined stainless steel tubing (Silcosteel, Restek, Bellefonte, Pennsylvania). With the valve array in sampling mode, the subsample flow passes through valves 1, 2, and 3 and the pretreatment traps and then into the sample trap mounted in the cold block (-80°C) where the target analytes are concentrated. Since the Valco valves employed (valves 1-4) have stainless steel internal surfaces, these valves were housed in a heated enclosure at 45°C in order to prevent condensation and subsequent

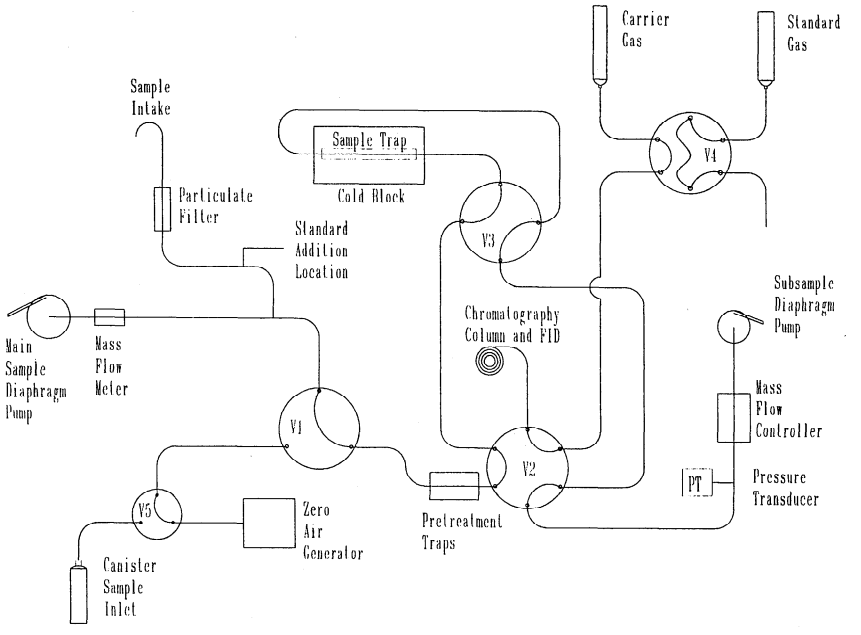

Figure 2. Flow paths for VOC measurement system shown in sampling mode.

losses. Noncondensible gases pass through the sample trap, through valves 3 and 2, past a pressure transducer and through a mass flow controller (MKS Instruments, Andover, Massachussets). Downstream diaphragm pumps (KNF Neuberger, Trenton, New Jersey) draw sample through both the main sample and subsample flow paths. In alternate valve arrays, valves 2 and 4 provide for carrier gas flow to the chromatography column and allow for periodic direct injection of a fixed volume of standard calibration gas by loading and injecting a microvolume loop installed across two ports of valve 4. Valve 5 (General Valve, Fairfield, New Jersey) provides for blank background determinations with zero-air from a zero-air generator (AADCO, Clearwater, Florida) and an inlet for canister or bag samples. Standard gases can also be diluted directly into the main sample flow. The sample handling and cold block assemblies are mounted on the top of the GC.

2.2.3. Sample collection scheme. This instrument has two channels and was designed to be easily adapted to any of three continuous in situ sampling schemes: relaxed eddy accumulation (REA) flux, gradient flux, or ambient concentration measurements. For this study, the system was configured to measure ambient concentrations of the widest possible suite of VOCs. Measurements were made continuously from a single height (9 m above the ground, ~6 m above the forest canopy), and the two measurement channels had different pretreatment systems and chromatography columns. The front column was a porous layer open tubular (PLOT) RT-Alumina 0.32 mm x 60 m (Restek, Bellefonte, Pennsylvania) and the rear column was a DB-WAX 0.32 mm x 60 m x 0.5 μm film thickness (J&W Scientific, Folsom, California) for the separation of less polar and more polar compounds, respectively. Pretreatment traps for the removal of water vapor (Nafion dryer, Perma Pure, Toms River, New Jersey), carbon dioxide and O_3 (Ascarite, Thomas Scientific, Swedesboro, New Jersey) were placed upstream of the preconcentration trap in the subsampling channel leading to the RT-Alumina column (see *Goldstein et al.* [1995a] for details). The Nafion dryer caused minor blank problems for 2-methylpropene, t-2-butene, and c-2-butene, which diminished slightly over time, but the traps did not affect any of the other compounds quantified on the RT-Alumina column (see below for discussion of MBO conversion to isoprene after drying samples in this measurement channel). An ozone trap (KI-impregnated glass wool, following *Greenberg et al.* [1994], conditioned before use at 150°C with ultra high purity (UHP) nitrogen flow overnight) was placed in the subsampling channel leading to the DB-WAX column (See Figure 2). All of these traps were effective throughout the measurement period without need for replacement.

Neohexane (10.08 ppm, Scott-Marrin, Riverside, California, certified National Institute of Standards and Technology (NIST) traceable +/- 2%) was added as an internal standard to the RT-Alumina channel by dynamic dilution continuously at 5 cm^3 s^{-1} STP (MKS Instruments, Andover, Massachusetts) to the main sample flow. Other standards were periodically added by dynamic dilution to the DB-WAX and RT-Alumina channel main sample flows for instrument calibration. The subsample flows for both channels were maintained at 20 cm^3 s^{-1} STP (MKS Instruments, Andover, Massachusetts). The sample traps (see section 2.2.5) were opened for 20 min and then isolated by switching valve 3, resulting in 400 mL samples (STP). Our samples represent 20 min averages of the ambient concentrations. While larger samples should improve the least detectable limit of the instrument, acquisition of ambient air samples larger than 400 mL led to flow anomalies associated with ice formation in the sample traps.

Chromatographic analysis was initiated by simultaneously switching valves 2 and 3 and heating the sample traps from -80°C to 250°C in 12 s with a nichrome wire heater. The trapped compounds were quickly desorbed into the helium carrier gas and carried onto the chromatography columns. Carrier gas flow was maintained and trap heating continued

for 60 s at 250°C to ensure complete desorption of the trapped compounds. Desorption was sufficiently fast to eliminate the need for cryofocusing.

Zero-air (AADCO) was introduced through valves 5 and 1 instead of ambient air every sixth run to check for VOC contamination in the measurement system.

2.2.4. Data acquisition and storage. Automation was accomplished using Hewlett-Packard (HP) Chemstation software and a Campbell Scientific data logger. We operated the measurement system with a sequence of Chemstation methods that controlled the GC parameters and eight additional electronic events. These events were used to count the individual GC runs, switch five electronic valves, and signal the desorption heater control circuitry.

Engineering data consisting of main and subsample flows, standard gas flows, support gas pressures, standard gas pressures, zero-air system pressures, trapping and desorption temperatures, heated valve enclosure temperature, and room temperature were acquired at 1 Hz and stored as 15 s averages using a CR10x data logger and AM416 multiplexer (both Campbell Scientific, Logan, Utah). At the beginning of each GC run, engineering data were downloaded from the data logger to the main computer.

2.2.5. Preconcentration system. The preconcentration system was designed to eliminate the need for liquid cryogen. Use of liquid nitrogen limits the range of field sites and the time periods for which VOC instruments may be easily deployed. Our preconcentration system simultaneously utilizes the physical process of condensation of analytes onto cold, inert surfaces and the chemical affinity of analytes for two different carbon-based adsorbents. The multistage solid adsorbent trap consists of 11 mg of graphitized carbon black (Carbopack B, 60/80 mesh, Supelco, Bellefonte, Pennsylvania) and 7 mg of carbon molecular sieve (Carbosieve SIII, 60/80 mesh, Supelco, Bellefonte, Pennsylvania) packed in series and held in place at each end by fused silica wool (untreated, Restek, Bellefonte, Pennsylvania), in a 10 cm long, 1/16 inch OD, 0.040 inch ID fused silica-lined stainless steel tube (Silcosteel, Restek, Bellefonte, Pennsylvania). The glass wool provides inert surface area for condensation of the least volatile compounds. The sample was loaded so that the less volatile compounds contact and are retained on the weaker adsorbents first and only the more volatile compounds reach the stronger adsorbent materials. The trap heater was an insulated nichrome wire wound around the fused silica-lined stainless steel tube and held in place by high-thermal conductivity epoxy (Omega Engineering, Stamford, Connecticut). Heating was controlled using proportional integral differential temperature controllers (Omega Engineering, Stamford, Connecticut) and thin wire type T thermocouples (Omega Engineering, Stamford, Connecticut). The trap and heater assemblies were mounted in an insulated aluminum block maintained at -80°C by a two-stage, sealed immersion cooler (Neslab, CC-100). The traps were configured to prevent

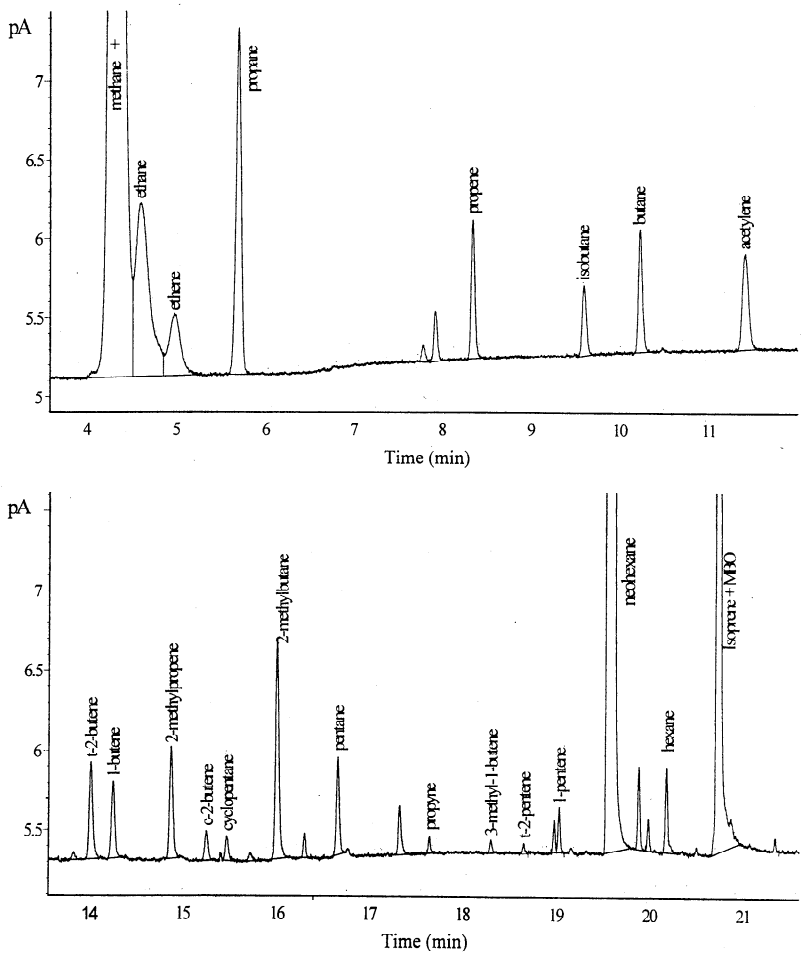

Figure 3. Sample chromatograms for (a) RT-Alumina PLOT column and (b) DB-WAX column.

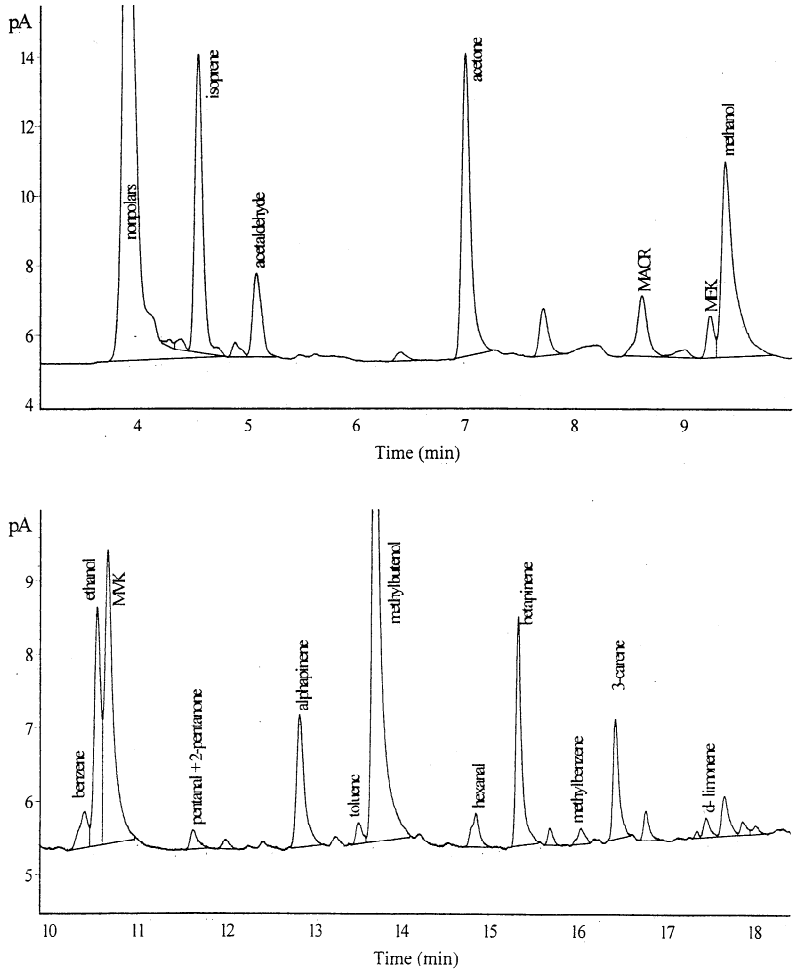

Figure 3. (continued)

breakthrough of target compounds, and the internal volume was minimized to permit rapid thermal desorption (-80°C to 250°C in 12 s). This eliminated the need to cryofocus the sample before chromatographic analysis. After sample injection the sample traps cool from 250°C to -80°C in less than 3 min and are then ready to collect new samples.

2.2.6. Chromatographic Separation. Chromatographic separation of the sampled gases was achieved with a two-channel Hewlett-Packard 6890 gas chromatograph (GC) with dual flame ionization detectors (FIDs). In the setup we deployed, the two sample pathways use a PLOT RT-Alumina column 0.32 mm x 60 m (Restek, Bellefonte, Pennsylvania) and a DB-WAX column 0.32 mm x 60 m x 0.5 μm film thickness (J&W Scientific, Folsom, California) for the separation of less polar and more polar compounds, respectively. Separation was optimized via oven temperature and carrier gas pressure programming. The GC was programed for a 37.2 min run time with a three-stage temperature program as follows: 34°C for 6 min, 5°C min^{-1} to 80°C, 12°C min^{-1} to 200°C, and hold at 200°C for 12 min. The two-stage carrier gas pressure program was as follows: 20 psi for 6 min, 1 psi min^{-1} to 45 psi, and hold at 45 psi for 6.2 min. This pressure and temperature programming allowed for optimized separation on both columns simultaneously. UHP helium which was further purified using moisture, hydrocarbon, and oxygen traps (J&W Scientific) was used as the carrier gas with a linear velocity of 23.2 cm s^{-1} through the RT-Alumina column and 25.3 cm s^{-1} through the DB-WAX column (based on column length divided by the average elution time of methane). Figures 3a and b show sample chromatograms from each column.

2.3. Sample Analysis

2.3.1. Quantification. Here we discuss the quantification of the RT-Alumina column and the DB-WAX column.

2.3.1.1. Rt-Alumina column: The RT-Alumina column was used to separate the low molecular weight (C_2-C_6) NMHCs, and concentrations were determined using a FID. (See Table 1 for a list of those compounds found to be separable, identifiable and quantifiable on the RT-Alumina column.) The linearity of FID response to NMHCs has been well established, and the response is roughly proportional to the weight percent of carbon atoms in the molecule [*Ackman*, 1968]. Quantification of a suite of target analytes was achieved by calculating a weighted response factor (RF_i) for each compound relative to a reference compound [*Ackman*, 1964]. Throughout this work, we used neohexane as the reference compound for the PLOT RT-Alumina column. Neohexane serves as an ideal internal standard because it is not naturally abundant, is stable in compressed gas standards at the ppm level, and is easily separated on this column.

Table 1. VOCs Found to Be Separable, Identifiable, and Quantifiable on the RT-Alumina Column

Compound	Blank, ppbv	RRF_i	R^2	n
Ethane*	0.017†	0.318	0.97	3
Ethene*	<LDL†	0.342	0.98	4
Propane*	<LDL	0.489	0.96	3
Propene*	0.034†	0.512	0.98	4
Isobutane	<LDL	0.659	na	na
Butane*	<LDL†	0.659	0.96	3
Acetylene*	<LDL	0.368	0.99	4
Cyclopentane	<LDL	0.854	na	na
Pentane*	<LDL	0.829	0.95	3
Propyne	<LDL	0.525	0.97	5
t-2-pentene	<LDL	0.853	0.99	4
c-2-pentene	<LDL	0.853	0.99	4
Neohexane	<LDL	1	na	na

Here, <LDL denotes below least detectable limit; RRF_i denotes weighted response factor for the individual compound relative to neohexane. (see section 2.3.1 for formulation); R^2 values are from calibration curves resulting from standard additions into real air throughout the measurement campaign; n denotes number of standard additions used in the calibration curve; and na denotes not available. Compounds with large blanks due to Nafion dryer contamination are t-2-butene, 2-methylpropene and c-2-butene.

*Always significantly above least detectable limit (LDL).

†Blanks for these compounds were higher for the first 1-2 weeks of peration due to using bottled zero-air, then decreased and stabilized at the value shown when zero-air generator was used.

The response factor for neohexane (RF_n) was determined according to the equation:

$$RF_n = (Fl_n / Fl_a)([\text{neohexane}] / \text{peak area}) \quad (1)$$

where Fl_n denotes the flow of neohexane standard (cm^3 s^{-1} STP), Fl_a denotes the flow of ambient air sample (cm^3 s^{-1} STP), [neohexane] denotes the concentration of the neohexane standard, and peak area denotes the integrated area of the neohexane peak. RF_n was calculated for each of the approximately 900 samples and was stable throughout the 30 day sample acquisition period with a relative standard deviation (RSD) of 5.8%.

Relative response factors (RRF_i) are calculated for each compound using the equation (adapted from *Goldstein et al.* [1995a])

$$RRF_i = (\text{mass}\%C_i)(\#C_i)/[(\text{mass}\%C_n)(\#C_n)] \quad (2)$$

where

$$\text{mass }\%C = 100\%(\#C_i)(12.01) / [(\#C_i)(12.01) + (\#H_i)(1.008)] \quad (3)$$

Here #C and #H refer to the number of carbon and hydrogen atoms in the molecule, respectively. Then

$$RF_i = RF_n/RRF_i \quad (4)$$

RF_i (ppb/peak area unit) multiplied by the integrated peak area yields concentration values for the individual compounds.

2.3.1.2. DB-WAX column: The DB-WAX column was used to separate more polar and larger VOCs, including OVOCs. (See Table 2 for a list of those VOCs found to be separable, identifiable, and quantifiable on the DB-WAX column.) Quantification of these compounds was complicated by the fact that FID response to OVOCs is not simply proportional to the number of carbon atoms in the compound. The functional groups that characterize these compounds (alcohols, aldehydes, and ketones) tend to suppress FID response [*Ackman*, 1968; *Blades*, 1973; *Scanlon*, 1985]. In order to determine empirical response factors (ppb/peak area), high-pressure ppm level gas standards (Scott-Marrin, Inc.) containing the target compounds were added by dynamic dilution into the main sample flow leading to the DB-WAX column on 7 nonconsecutive days throughout the 30 day sample acquisition period. Background concentrations during the standard additions were estimated from the average of the concentrations immediately before and after the standard additions. These additions of standards into real air samples allowed assessment of the entire analytical system's response to individual compounds. Table 3 lists empirically determined RFs for compounds separated on the DB-WAX column.

To determine concentrations of oxygenated compounds for which quantitative standards were not available, we derived RFs using two theoretical methods. The first method relies on a mass-weighted response (referred to as RF_{im}) similar to that described for the PLOT RT-Alumina column (equations (1)-(4)); however, we included oxygen (#O) in the calculation of mass %C:

$$\text{mass }\%C = 100\%(\#C_i)(12.01) / [(\#C_i)(12.01) + (\#H_i)(1.008) + (\#O_i)(15.99)] \quad (5)$$

The second theoretical method derived RFs from effective carbon numbers (ECNs). The ECN concept was introduced to explain observed FID responses to organic compounds which contained functional groups (such as alcohols or ketones) where $ECN_{compound}$ equals the number of carbon atoms in the molecule minus a correction factor (*Sternberg et al.*, 1962). Recent work provides correction factors of 0.6 for alcohols and 0.8 for aldehydes and ketones [*Apel et al.*, 1998a; *Jorgensen et al.*, 1990]. The ECN RF (referred to as RF_{ie}) was derived from the empirically derived RF for isoprene (RF_{isop}), as follows:

$$RF_{ie} = (RF_{isop})(ECN_{compound}) / (ECN_{isop}) \quad (6)$$

Table 2. VOCs Found to Be Separable, Identifiable, and Quantifiable on the DB-WAX Column

Compound	Blank, ppb	R^2	n	RSD_{slope}, %
Isoprene	0.045	0.99	8	2.1
Acetaldehyde	0.563	0.95	7	3.9
Acetone	0.132	0.92	7	5.4
Methacrolein	<LDL	0.96	9	2.8
Methyl ethyl ketone	<LDL	0.97	9	2.8
Methanol	0.823	0.61	7	11.5
Methyl vinyl ketone	0.127	na	na	na
Pentanal	<LDL	0.97	11	2.3
2-Pentanone	<LDL	0.97	11	2.3
Alpha-pinene	<LDL	0.97	6	1.1
Toluene	<LDL	na	na	na
Methylbutenol	<LDL	0.91	5	3.7
Hexanal	<LDL	0.93	11	2.8
3-Carene	<LDL	0.99	7	3.3
D-limonene	<LDL	0.95	4	5.8

Here, <LDL denotes below the least detectable limit; na denotes not available; n denotes number of standard additions used in the calibration curve; R^2 value is from calibration curves resulting from standard additions into real air; and RSD_{slope} is the relative standard deviation of the slope of the calibration curves resulting from standard additions into real air.

Table 3. Quantification Parameters for the DB-WAX Column

Compound	Standard Mix	Empirical RF	Derived RF_{im}*	Derived RF_{ie}†	Ratio RF/RF_{im}	Ratio RF_{im}/RF_{ie}
Isoprene	a,d,e	0.0350‡	0.0350	0.0348	1.00	1.004
Acetaldehyde	a,e	0.0946§	0.1413	0.145	0.67	0.97
Acetone	a,e	0.0856‡	0.0828	0.0791	1.03	1.05
Methacrolein	a,e	0.0677§	0.0562	0.0544	1.20	1.03
Methyl ethyl ketone	e	0.071§	0.0578	0.0543	1.23	1.06
Methanol	e	0.243§	0.411	0.435	0.59	0.94
Methyl vinyl ketone	···	na	0.0562	0.0544	na	1.03
Pentanal+2-pentanone	e	0.0459§	0.0442	0.0414	1.04	1.07
Alpha-pinene	a,b	0.0185	0.0175	0.0174	1.06	1.00
Toluene	···	na	0.0241	0.0249	na	0.97
Methylbutenol	c	0.0409	0.0442	0.0396	0.93	1.12
Hexanal	e	0.047§	0.0357	0.0335	1.32	1.07
3-Carene	b	na	0.0175	0.174	na	1.00
D-limonene	b	na	0.0175	0.174	na	1.00

Here, na denotes not available; a denotes six component mix from Scott-Marrin, National Institute of Standards and Technology (NIST) traceable +/-2%; b denotes four component mix from Scott-Marrin, not quantitatively certified; c denotes single-component methylbutenol standard from Scott-Marrin, NIST traceable +/-2%; d denotes single component isoprene standard from Scott-Marrin, NIST traceable +/-2%; and e denotes fourteen component mix from Eric Apel at National Center for Atmospheric Research (NCAR), concentrations provided by NCAR (mix prepared by Scott-Marrin but not quantitatively certified).

*Derived from mass %C relative to isoprene. (see section 2.3.1 for formulation.)

†Derived from effective carbon number (ECN) ratios relative to (see section 2.3.1 for formulation.)

‡Used RF values derived from Scott-Marrin mix a. Concentrations in the NCAR mix e were 14% higher for acetone, 37% higher for methacrolein, 5% higher for isoprene, and 38% lower for acetaldehyde than the concentrations in the Scott-Marrin mix.

§Used theoretically derived RF_{im} in lieu of empirically-derived RFs for these compounds. Available standards were only accurate to +/- 5% and +/- 10% for acetaldehyde and methacrolein, respectively; other compound standards exhibited internal inconsistencies or were not quantitatively certified.

Table 3 compares these two approaches for determining response factors against empirically derived response factors. With two exceptions (acetaldehyde and MBO), the weighted mass percent carbon derivation resulted in RFs that were closer to the empirically determined RFs than were the ECN RFs. The ratio RF_{im} / RF_{ie} shows that the RFs derived via the two theoretical methods are within 12% of each other (and often closer) for all compounds reported here. An advantage of the weighted mass percent carbon approach is that RF can be derived theoretically for any VOC or OVOC without relying on published ECN correction factors. In any case, these theoretical estimates of RF will only be valid for compounds that are sampled and analyzed without any losses in the analytical system.

2.3.2. Data reduction. Chromatographic data from the FIDs were integrated using HP Chemstation software on a personal computer. Peak identification was achieved by direct injection and standard addition of single- and multiple-component gas standards (Scott-Marrin and Scott Specialty Gases). Prominent peaks were selected as reference peaks to create retention time indices. Methane, propane, acetylene, and neohexane were used as retention time reference compounds on the RT-Alumina column. Nonpolar compounds (coeluted with methane), acetone, and MBO were used as retention time reference compounds on the DB-WAX column. Chromatograms from the PLOT column were routinely analyzed using HP Chemstation automated integration and identification methods. Chromatograms from the DB-WAX column required significantly more attention due to coeluting peaks, peak tailing, and a less stable baseline, and thus were all integrated by hand.

2.3.3. Detection limits. Detection limits were defined as chromatography peaks whose amplitude was ~3 times baseline noise. Based on analysis of the smallest detectable peak in real air samples, detection limits were typically 6-8 pptv, with slightly higher limits for partially coeluting compounds. In general, detection limits were lower on the RT-Alumina column than on the DB-WAX column because the chromatography was cleaner (see sample chromatograms in Figures 3a and b).

2.3.4. Precision. Precision for the sampling channel leading to the RT-Alumina column was demonstrated by repeated analyses of neohexane standard additions in the field. Instrument response was stable for each of the approximately 900 samples taken throughout the 30 day sample acquisition period with an RSD of 5.8%. Precision for the sampling channel leading to the DB-WAX column is expressed in Table 2 as the relative standard deviation of the slope (RSD_{slope}) of the calibration curves resulting from a series of standard additions into real air performed throughout the measurement period.

2.3.5. Accuracy. The accuracy of these measurements is limited mainly by the accuracy of available standards, the integrity of the target compounds in the sampling and analysis system, and knowledge of the response of the FID to the individual target compounds.

The instrument response and the integrity of the target compounds in the sampling and analysis system is best examined by dynamic dilution of standards into real air through the entire sampling system under field measurement conditions. A series of standard additions were performed throughout the measurement period. Standards were added both at the inlet and near the outlet of the sampling tubes to check for losses on the particle filters and in the tower-to-instrument sampling tubes. No significant losses were observed in the sampling system transfer tubing.

Interconversion of MBO to isoprene was observed after drying the sample in the preconditioning system leading to the RT-Alumina column. The dehydration probably occurred on the trapping matrix as the samples were heated for injection into the chromatography column. This interconversion phenomenon, as observed by *Goldan et al.* [1993], was verified in our system by simultaneously acquiring identical air samples from isoprene- and MBO-enriched streams of ambient air and delivering these samples to both columns. No interconversion of MBO to isoprene occurred on the nondried channel leading to the DB-WAX column; thus isoprene and MBO are reported only for the DB-WAX channel.

The largest uncertainties in reported concentrations are for the oxygenated compounds. These uncertainties are mostly due to the quality of the standards and potentially due to losses in the preconditioning traps, sampling traps, or chromatography columns. Four compounds (acetaldehyde, acetone, isoprene, and methacrolein) were in two of the high-pressure standard cylinders prepared by Scott-Marrin; one was quantified at NCAR (OVOC1 by *Apel et al.* [1998a]), and the other was certified by Scott-Marrin. We found significant differences between these two high-pressure standard cylinders for acetaldehyde (38%), acetone (15%), isoprene (6%), and methacrolein (37%). The accuracy of our measurements of these compounds is similar to published reports [*Farmer et al.*, 1994: *Montzka et al.*, 1995; *Goldan et al.*, 1997; *Singh et al.*, 1995], and recent work by *Apel et al.* [1998b] revealed similar difficulties in calibrating measurement systems for oxygenated compounds. It is clear that more work needs to be done to create reliable standards for oxygenated compounds and improve our understanding of the FID response to them. More reliable standards would enable us to better account for potential losses of these important compounds in our measurement systems and thereby improve their accuracy.

One measure of the accuracy of this analytical system for individual compounds is the ratio between empirically determined and theoretically derived RFs. Table 3 shows this ratio for compounds where quantitative gas standards were available. Methanol response showed the largest disagreement between $RF_{empirical}$ and RF_{im} (41%). The same ratio for acetaldehyde, hexanal, methyl ethyl ketone, and methacrolein showed disagreements of 33%, 32%, 23%, and 20%, respectively. The balance of the compounds showed disagreements between RF and RF_{im} of 7% or less. These differences could be due to inaccurate standards, inaccurately derived RFs, or measurement problems, but they do provide a conservative estimate of the accuracy achieved by this measurement system.

3. Blodgett Forest Experiment

3.1. Identification of Source Types

In this section the measured VOCs are categorized into source groups based on factor analysis of the full VOC data

Table 4. Factor Analysis Results for Full VOC Data Set

	Loadings (Values < 0.3 omitted)					
Compound	Factor 1	Factor 2	Factor 3	Factor 4	Factor 5	Factor 6
Ethane	0.73				0.35	
Ethene	0.35			0.86		
Propane	0.91					
Propene		0.33		0.76		0.40
Isobutane	0.94					
Butane	0.99					
Acetylene	0.76	0.41				
Cyclopentane		0.71				
Pentane	0.92					
Propyne	0.34	0.75				
t-2-pentene				0.43		
c-2-pentene						
Isoprene		0.38				0.65
Acetaldehyde		0.56	0.33	0.31		
Acetone	0.39	0.39			0.71	
MACR		0.87				0.40
MEK	0.49			0.39	0.61	0.35
Methanol		0.57	0.36		0.50	
MVK	0.36	0.72				
Pentanal + 2-pentanone	0.34		0.33	0.37	0.60	
Alpha-pinene			0.94			
Toluene	0.68	0.45				
Methylbutenol				0.32		0.70
Hexanal	0.37		0.59		0.50	
3-Carene			0.91			
D-limonene			0.90			
Importance of factors						
Sum square loadings	6.32	4.15	3.55	2.45	2.32	1.76
Proportion of variation	0.24	0.16	0.14	0.09	0.09	0.07
Cumulative variation	0.24	0.40	0.54	0.63	0.72	0.79

Factor analysis was performed in SPLUS 4.5 (MathSoft, Inc.), using varimax rotation and maximum likelihood estimation. The model was limited to six factors because additional factors did not have significant sum square loadings (less than 0.5), and did not explain a significant portion of the variation (less than 0.02). Proportion variation defines the fraction of data explained by each factor. Cumulative variation is the sum of the proportion variation, indicating that these six factors explain 79% of observations.

Table 5. Categories of VOCs Based on Factor Analysis of Full Data Set

Factor	Compounds
Factor 1: athropogenic emissions	butane, isobutane, pentane, propane, acetylene, ethane, toluene
Factor 2: biogenic emission oxidation products	methacrolein, propyne*, methyl vinyl ketone, cyclopentane*
Factor 3: Temperature (not light) dependent biogenic emissions	alpha-pinene, 3-carene, d-limonene, hexanal
Factor 4: Anthropogenic emissions plus light dependent biogenic emissions	ethene, propene
Factor 5: Anthropogenic emission and oxidation products plus biogenic emissions	acetone, methyl ethyl ketone, pentanal+2-pentanone
Factor 6: Temperature and light dependent biogenic emissions	methylbutenol, isoprene

Compounds associated with each factor are listed in order of importance down to loadings of 0.6. Names of factor categories were prescribed based on previous knowledge of sources and observed temporal patterns for the primary compounds associated with that factor.

*Maximum propyne concentrations were 0.02 ppbv, and maximum cyclopentane concentrations were 0.05 ppbv. The association of these low-concentration compounds with isoprene oxidation products methacrolein and methyl vinyl ketone could potentially be due to coelution with other minor isoprene oxidation products.

set (26 compounds, excluding environmental parameters such as wind, temperature, light, and time). Factor analysis statistically groups variables into larger-order factors based on the correlation between observed variables. Results of the factor analysis are described below; then examples of observed concentration patterns are used to suggest the sources driving each factor (or group of VOCs).

Factor analysis was performed in SPLUS 4.5 (MathSoft, Inc.), using varimax rotation and maximum likelihood estimation (results in Table 4). Six factors were extracted, accounting for a total of 79% of the variation in the observations. The analysis was limited to six factors because additional factors did not explain a significant additional portion of the variation (less than 2%). Standardized variables are linearly related to each factor with loading coefficients. Compounds associated with each factor are listed in order of importance down to loadings of 0.6 in Table 5. Maximum possible loading on each factor is 1, and loadings below 0.3 were not reported because they are considered insignificant for this analysis. Loadings between 0.3 and 0.6 suggest a weak association with the factor.

The factor analysis successfully differentiated compounds which were solely anthropogenically emitted (factor 1: butane, isobutane, pentane, propane, acetylene, ethane, toluene), solely biogenically emitted (factors 2, 3, and 6), or emitted from a combination of biogenic and anthropogenic sources (factors 4 and 5). Solely biogenically emitted compounds were differentiated into oxidation products of biogenic emissions (factor 2: methacrolein and methylvinylketone), temperature (not light) dependent emissions (factor 3: terpenes), and light and temperature dependent emissions (factor 6: methylbutenol and isoprene). Compounds which were emitted from a combination of biogenic and anthropogenic sources were separated into anthropogenic emissions plus light dependent biogenic emissions (factor 4: ethene and propene), and anthropogenic emission and oxidation products plus biogenic emissions (factor 5: acetone, methylethylketone, pentanal+2-pentanone). These factor names were prescribed based on previous knowledge of sources and the observed temporal patterns for the primary compounds as described below.

To further examine the sources driving each factor, observed environmental variables (wind speed and direction, air temperature, and PAR, Figure 4) and concentration patterns (Figure 5) are presented from July 12 to 15, 1997. The diurnal variation in wind speed and direction (Figure 4a) was remarkably consistent throughout the whole measurement period. Predominant day time winds were upslope from the Sacramento valley to the west, generally bringing polluted air masses to the site beginning around noon. At night the flow reversed directions, bringing air downslope from the Sierra Nevada mountains to the east. This diurnal cycle of wind direction was closely coupled to changes in wind speed, with higher wind speeds during the day and lower wind speeds at night. Diurnal patterns of air temperature and photosynthetically active radiation (PAR) were quite consistent from day to day (Figure 4b). There were no clouds from July 12 to 15. The temporal patterns in wind, PAR, and temperature were correlated with the variability of observed VOC concentrations and suggest information about their sources.

Compounds associated with factor 1 ("anthropogenic emissions") included butane, isobutane, pentane, propane, acetylene, ethane, and toluene. These compounds were all highly correlated and are known to have dominantly anthropogenic sources in northern midlatitudes [*Goldstein et al.*, 1995b]. The temporal pattern of butane concentration (Figure 5a) was representative of the whole group. Butane concentration began to increase rapidly around noon after the wind had shifted direction and wind speed had increased, bringing polluted air to the measurement site from the valley below. Butane concentration typically remained high until cleaner air descended from above during the night, and butane decreased to its lowest concentration in the morning.

Ethene had a remarkably similar temporal pattern to butane, suggesting a dominantly anthropogenic source (Figure 5a), however ethene (and propene) loaded highly on factor 4 rather than factor 1. A close inspection of the data reveals that ethene (and propene) increased in the morning when the Sun rose after 0600 hours, indicating a local light dependent biogenic source. *Goldstein et al.* [1996] reported similar biogenic emissions of ethene and propene from a deciduous forest. In the early morning, local light-driven biogenic emissions would be most apparent because the vertical mixing rates were low and anthropogenic emissions from the valley below had not yet reached the site. This differentiation between factor 1 ("anthropogenic emissions") and factor 4 ("anthropogenic emissions plus light dependent biogenic emissions") provides a good example of the usefulness of factor analysis for understanding observations of VOCs.

All of the terpenes measured in this study (α-pinene, 3-carene, d-limonene) loaded highly on factor 3 ("temperature (not light) dependent biogenic emissions"). Terpenes (represented by α-pinene in Figure 5b) had a distinct diurnal pattern

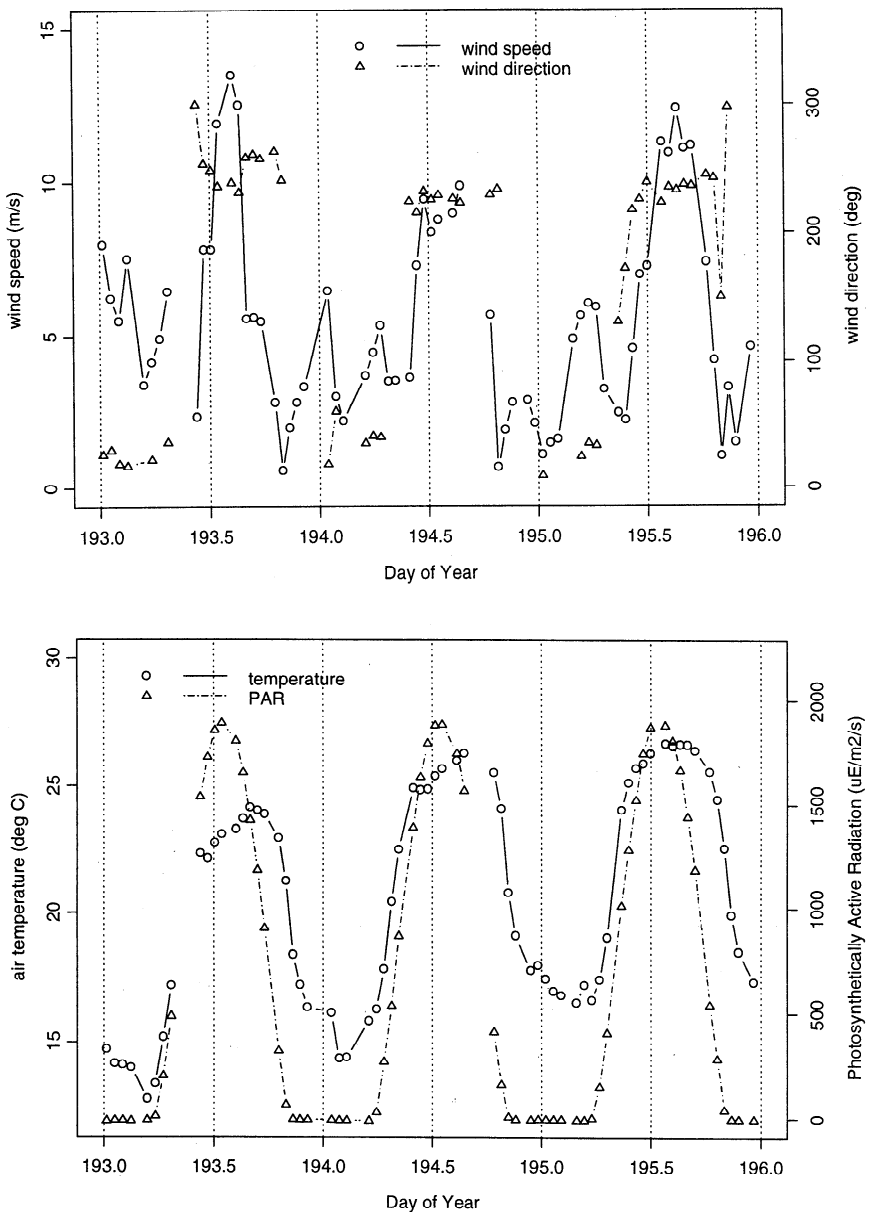

Figure 4. Environmental parameters affecting observed concentrations of VOCs from July 12-15, 1997, including (a) wind speed and direction and (b) air temperature and photosynthetically active radiation.

with highest concentrations observed at night when vertical mixing was weakest, and lowest concentrations during the day when vertical mixing was most vigorous. This pattern is consistent with continuous temperature-driven biogenic emissions. Hexanal also loaded highly on factor 3, suggesting that hexanal concentrations can at least partially be attributed to temperature (and not light) dependent biogenic emissions.

Isoprene and MBO both loaded highly on factor 6 ("light and temperature dependent biogenic emissions"). Both compounds had clear diurnal cycles (Figures 5c and d) with maximum concentrations in the afternoon and minimum concentrations in the early morning. Midday concentrations were lower on day 193 than on 194-195 when the air temperature was also lower. These observations are all consistent with their light- and temperature-driven source. MBO concentrations increased earlier in the morning than isoprene (particularly days 194-195), suggesting a different source footprint. MBO was emitted directly from the pine trees surrounding the measurement site [*Harley et al.*, 1998]. One local source of isoprene was black oak trees (*Quercus kellogii*) which were present at a 3-7% composition level throughout the mixed conifer forest immediately surrounding the site (F. Schurr, personal communication, 1998). This local source is evident as a slight increase in isoprene concentration coincident with the morning increase in MBO and α-pinene on day 195 when vertical mixing was still weak and the wind direction had not yet shifted. This was not the primary source of isoprene. Generally, isoprene concentrations rose sharply when wind shifts brought air masses from the southwest foothills a few hours later, where a band of oak trees constitutes a large source of isoprene.

MVK and MACR both loaded highly on factor 2 ("Biogenic emission oxidation products"). The sum of the major isoprene oxidation products MVK and MACR (Figure 5c)

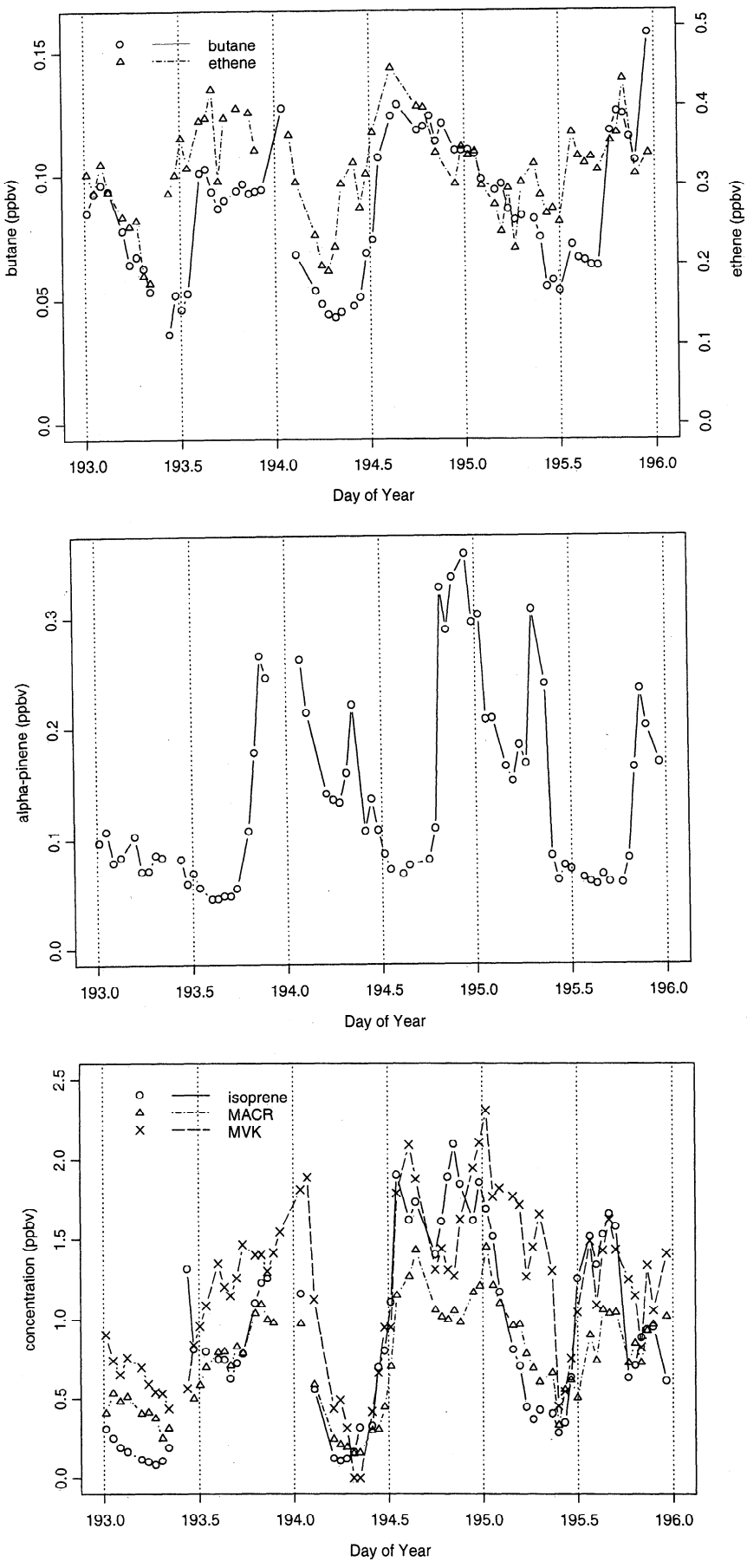

Figure 5. Observed concentration of VOCs from July 12-15, 1997, including (a) butane and ethene, (b) α-pinene, (c) isoprene, methacrolein, and methyl vinyl ketone, and (d) methylbutenol and acetone.

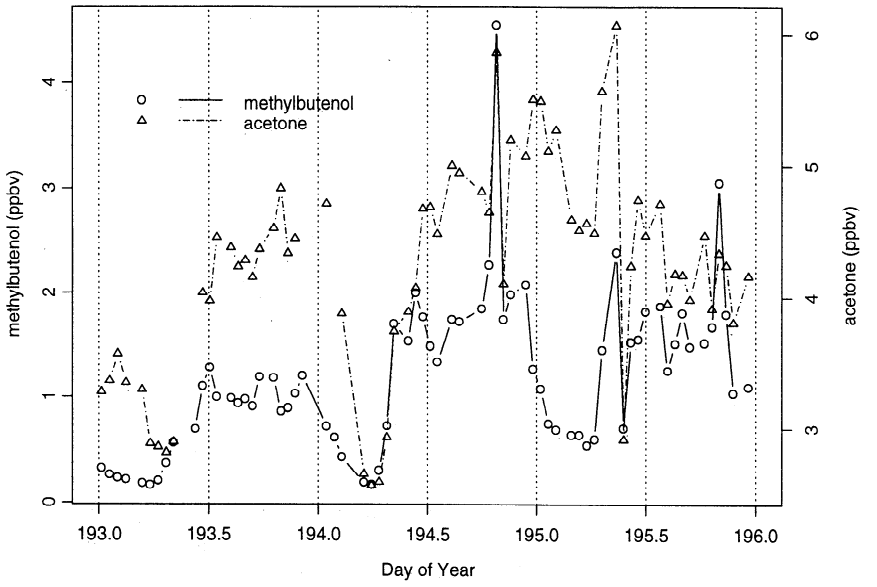

Figure 5. (continued)

was typically twice the isoprene concentration in the afternoon, suggesting a source distant enough to allow for photooxidation of at least 2/3 of the isoprene during transport. Thus, we conclude that almost all of the isoprene was emitted from the oak trees that are 30-50 km downhill. It is interesting that factor analysis showed isoprene to be more closely related to MBO (consistent emission drivers of temperature and light, but emitted from different geographical locations) than to isoprene's oxidation products. MVK and MACR generally arrive at the measurement site together with isoprene, but have different photochemical behavior and thus their concentrations lagged isoprene slightly.

Acetone loaded highly on factor 5 ("anthropogenic emission and oxidation products plus biogenic emissions") along with MEK and pentanal+2-pentanone (peaks were not separated on chromatogram). Acetone may be a direct emission from combustion, an oxidation product, or a direct biogenic emission [*Singh et al.*, 1994]. At least two if not three of these source categories are evident in the data from July 12-15, 1997 (Figure 5d). Acetone concentration increased with light in the morning coincident with MBO, and increased again coincident with butane when the wind shifted, carrying anthropogenic emissions upslope from the valley below (these patterns are particularly clear during day 194). This temporal pattern indicates influences from both anthropogenic and biogenic sources, but does not clearly show whether acetone is an anthropogenic oxidation product or a direct emission. MEK and pentanal+2-pentanone varied temporally like acetone, suggesting a similar combination of sources.

The influence of biogenic emissions on many of the compounds shown in Figure 5 was particularly apparent during a 2 hour window on the morning of day 195. The wind speed and vertical mixing rates were low, and anthropogenic emissions from the valley below had not yet reached the site as shown by the butane concentration. At this time, there was a large coincident increase observed for all the locally emitted biogenic compounds, including α-pinene, MBO, acetone, and ethene, and a small increase for isoprene. Similarly, there were increases of acetaldehyde and methanol in the morning coincident with MBO, suggesting some local biogenic emission for these compounds.

Among the anthropogenic VOCs (AVOCs) measured at this site, ethane, acetone, and methanol were found in greatest abundance; however, acetone and methanol probably had significant biogenic sources as well. Among the dominantly biogenic VOCs (BVOCs), MBO was typically the most abundant with slightly higher concentrations than isoprene. Among the terpenes, 3-carene was found in greater abundance than either α-pinene or d-limonene, but all three were found in low abundance relative to MBO or isoprene.

3.2. VOC and OVOC Contributions to OH Loss at Blodgett Forest

In order to assess the relative impact of AVOCs and BVOCs on the photochemistry of the troposphere at this site, we calculated the contribution of all measured compounds from 1100 to 1600 (when O_3 production is most vigorous) to the OH loss rate ([VOC] x k_{OH}) as a simple indicator of photochemical activity. Daytime mean concentrations for all measured compounds were calculated for five time periods: the entire month, the single cleanest and dirtiest days, and the coolest and hottest days (Table 6). Relative OH radical loss rates for each time period are shown in Figure 6. The vertical bars represent the percent contribution to the OH radical loss rate for the conditions stated. During daytime mean conditions the BVOCs (including the terpenes, isoprene, MACR, MVK, MBO) accounted for 70% of OH radical loss rate, with isoprene and its primary oxidation products, MVK and MACR, contributing 45% of the total. MBO accounted for 21% of the total. The terpene group (alpha-pinene, 3-carene, d-limonene) contributed only 4%. Acetaldehyde dominated the anthropogenic contribution at 6%, though some of the acetaldehyde may be attributable to biogenic emissions. The anthropogenic group (sum of all other AVOCs measured at this site) was only 3% of the total. These results compare closely to a recent [*Goldan et al.*, 1997] assessment of the contribution of a similar group of compounds to the OH radi-

Table 6. Mean Daytime (1100-1600) Concentrations (ppbv) and *k* Constants

Compound	July	Cold Day	Hot Day	Clean Day	Dirty Day	k, cm^3 $molecules^{-1}$ s^{-1}
Ethane	0.951	0.792	0.947	0.875	1.705	2.68E-13
Ethene	0.311	0.284	0.325	0.270	0.311	8.38E-12
Propane	0.356	0.249	0.532	0.161	1.035	1.15E-12
Propene	0.114	0.075	0.116	0.078	0.062	2.56E-11
Isobutane	0.037	0.026	0.056	0.015	0.137	2.34E-12
Butane	0.073	0.049	0.104	0.030	0.243	2.54E-12
Acetylene	0.192	0.150	0.306	0.108	0.353	9.00E-13
Cyclopentane	0.018	0.011	0.016	0.009	0.020	5.16E-12
Pentane	0.047	0.036	0.072	0.023	0.115	3.94E-12
Propyne	0.006	0.003	0.013	0.000	0.007	5.90E-12
t-2-pentene	0.001	0.000	0.001	0.004	0.000	3.19E-11
c-2-pentene	0.001	0.000	0.000	0.000	0.000	3.19E-11
Isoprene	1.075	0.505	2.069	0.544	0.320	1.01E-10
Acetaldehyde	1.313	0.753	1.761	0.705	1.610	1.53E-11
Acetone	4.395	2.592	6.035	2.279	4.678	2.26E-13
MACR	0.601	0.378	0.970	0.358	0.376	3.35E-11
MEK	0.294	0.174	0.340	0.171	0.332	1.15E-12
Methanol	10.36	7.274	9.351	4.736	6.378	9.32E-13
MVK	1.124	0.788	1.675	0.680	0.496	1.88E-11
Pentanal + 2-pentanone	0.067	0.026	0.078	0.038	0.060	2.85E-11
Alpha-pinene	0.051	0.027	0.067	0.026	0.025	5.37E-11
Toluene	0.043	0.038	0.049	0.024	0.061	5.96E-12
Methylbutenol	1.254	0.704	1.822	0.614	0.577	5.40E-11*
Hexanal	0.048	0.033	0.061	0.026	0.035	2.50E-11†
3-Carene	0.064	0.040	0.057	0.034	0.039	8.8E-11
D-limonene	0.021	0.015	0.032	0.009	0.019	1.7E-10

Here, k denotes reaction constant for oxidation by OH radical; source is *Atkinson* [1989] except where noted. Read 2.68E-13 as 2.68×10^{-13}.

*Rudich et al. [1995], at 299 K.

†Averaged between butanal and pentanal from *Atkinson* [1989].

cal loss rate at Idaho Hill in the Rocky Mountains of Colorado.

Other contributors to OH radical reactivity at this site include benzene, ethanol, m-, p-, and o-xylene, CO and CH_4. Although benzene, ethanol, and the xylenes were not measured quantitatively, our qualitative assessment of their abundance and subsequent consideration of their OH radical reactivity indicate their contribution to overall OH radical reactivity to be <1%. CO and CH_4 levels were not measured at our site but were assumed to be similar to California Air Resources Board (CARB) July 1995 Placerville monitoring station data [CARB, 1996] with average values for CO and CH_4 of 200 and 1700 ppbv, respectively. These estimated CO and CH_4 values were incorporated into all OH radical

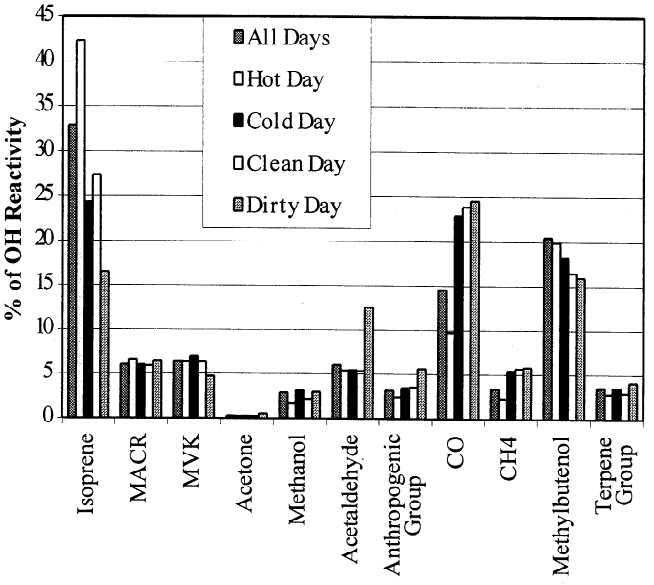

Figure 6. Relative OH radical reactivities (including values for CO and CH_4 estimated from California Air Resources Board data) for the whole measurement period July 2 through August 1, 1997, the cleanest day (July 10, 1997), the dirtiest day (July 13, 1997), the coolest day (July 17, 1997), and the hottest day (July 20, 1997).

reactivity calculations, and in each of the cases biogenic VOCs still dominated OH radical reactivity. By comparison, *McKeen et al.* [1997] measured 14 additional anthropogenic contributors to OH radical reactivity at their Colorado site. The cumulative reactivity of all but formaldehyde was less than 1.7% of their reported total. Formaldehyde accounted for 12.7% of OH losses under low-NO_x (<0.5 ppbv) conditions [*McKeen et al.*, 1997]. We expect that formaldehyde would contribute a similar amount to the OH reactivity at Blodgett Forest.

The regular air transport patterns at this site allowed us to examine the impact of "clean" and "dirty" air masses on OH radical reactivity. The cleanest day (Day 191) and dirtiest day (day 194) were determined from concentrations of the AVOCs identified in factor 1. The dirtiest day occurred during flow from the southeast and was not typical of air quality or wind direction at this site. In terms of concentration alone, the AVOCs in that air mass had concentrations 2-3 times higher than the monthly mean values. Even under these most polluted conditions, the BVOCs still accounted for 47% of OH radical loss rate, with MBO being equal to isoprene at 16% each. The terpene group contribution was 3% on the clean day and 4% on the dirty day. Interestingly, MVK and MACR contributions were essentially the same for clean and dirty days, possibly indicating accelerated oxidation of isoprene in the polluted air mass, or a longer travel time from the isoprene source. BVOC contribution to the total OH loss rate on the cleanest day (59%) was smaller than the monthly mean case (70%). The AVOC contributions (excluding CO and CH_4) essentially doubled from the clean day to the dirty day, mostly due to increases in acetaldehyde, suggesting large photochemical production or direct anthropogenic emission of this compound.

3.3. Temperature Dependence of OH Radical Reactivity

The effect of temperature on the relative contribution of AVOCs and BVOCs to the OH radical loss rate at this site was initially assessed by comparing the single coldest and hottest days of the measurement period. On the cold day (day 198), BVOCs accounted for 60% of the total OH radical loss rate, with isoprene and its oxidation products, MACR and MVK, accounting for over half of the BVOC contribution. On the hottest day (day 201), BVOCs accounted for 79% of the total OH radical loss rate.

One would predict a strong exponential relationship between daytime air temperatures and total OH radical loss rates because MBO and isoprene emissions are exponentially dependent on temperature, and both are highly reactive. That relationship is clearly evident over the whole measurement period at this site (Figure 7, Table 7). In fact, temperature is the single most important factor determining total OH loss rates at this site, with OH loss rates doubling over roughly a 4°C temperature increase. Figure 7 shows the relationship between air temperature and OH radical loss coefficients for the days when complete data sets were available for all compounds. The correlations between OH reactivity, biogenic VOC emissions, and temperature strongly suggest that on the hottest days of the summer when ozone concentrations are highest, biogenic VOCs are dramatically more important than anthropogenic VOCs for regional ozone production in the Sierra Nevada mountains, even at our site ~75 km downwind of Sacramento.

4. Conclusions

We designed, built, and deployed a fully automated system to measure ambient concentrations of C_2-C_{10} VOCs, including many oxygenated compounds, with high temporal resolution from July 2 to August 1, 1997. This system allowed us to measure alkanes, alkenes, alkynes, aromatics, alcohols, ketones, aldehydes, terpenes, and isoprene and its oxidation products to low pptv levels in a remote forested ecosystem. These in situ measurements had little or none of the interconversions or artifact formation normally associated with canister or cartridge sampling and did not require the use of liquid cryogen.

Factor analysis allowed for source categorization of the measured compounds. Among the anthropogenic VOCs measured at this site, ethane, acetone, and methanol were

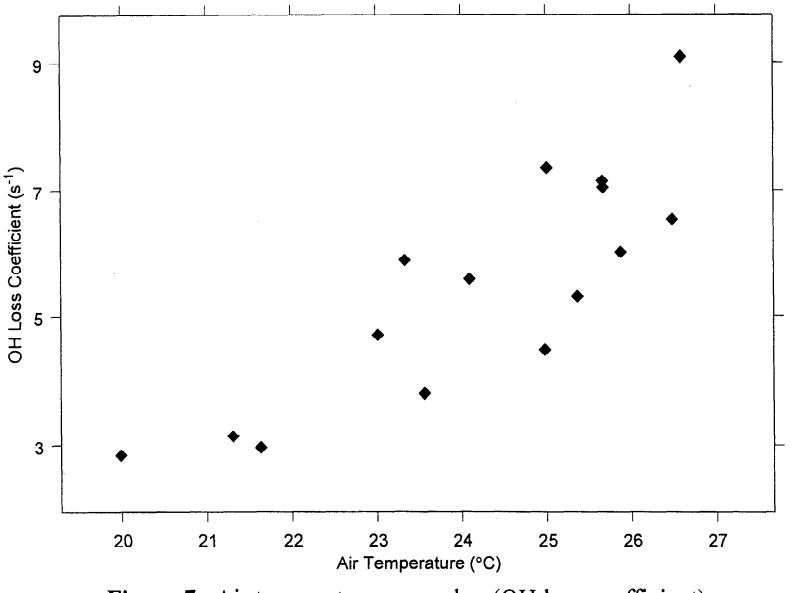

Figure 7. Air temperature versus log (OH loss coefficient).

Table 7. Total OH Radical Loss Coefficients and Mean Daytime Air Temperatures for the Whole Sampling Period, and Cold, Hot, Clean, and Dirty Days

	Total OH Radical Loss Coefficient, s^{-1}	Mean Daytime Air Temperature, °C
All July	5.58	24.54
Cold day	3.08	21.31
Hot day	9.02	26.58
Clean day	2.92	21.63
Dirty day	2.77	19.99

found in greatest abundance; however, acetone and methanol probably also had significant biogenic sources. The factor analysis and observed temporal patterns indicated acetone, ethene, propene, methanol, hexanal, and acetaldehyde all had both biogenic and anthropogenic sources. VOCs which were clearly of biogenic origin included MBO, the terpenes, and isoprene and its oxidation products, MVK and MACR. Among the BVOCs, methylbutenol was typically found in highest concentration, followed closely by isoprene. Among the terpenes, 3-carene was found in greater abundance than either α-pinene or d-limonene, but all three were in significantly lower abundance than isoprene.

The relative impact of AVOCs and BVOCs on the oxidative capacity of the troposphere at this site was assessed. Total OH radical loss rates were exponentially related to air temperature. Throughout the entire month and for the coldest and hottest, and cleanest and dirtiest days, BVOCs were found to dominate OH radical loss rates, with isoprene providing the largest biogenic VOC contribution in all cases. MBO, an alcohol not measured in most past studies, proved to be extremely significant for regional photochemistry, with OH radical loss rates ranging from 16% to 21% of the total. Acetone was not a significant compound in terms of its OH reactivity at this site. However, given its abundance and its relatively long atmospheric lifetime, biogenic emission of acetone from sites such as this may have implications for atmospheric chemistry beyond the regional scale.

It is clear from this work that by the time urban air masses arrive at 1315 m elevation, roughly 75 km downwind of Sacramento, VOC photochemistry is dominated by biogenically emitted compounds. More research is needed to determine biogenic emission rates and the factors controlling them for MBO, terpenes, ethene, propene, acetone, hexanal, acetaldehyde, and methanol from these pine ecosystems in order to understand their importance for regional photochemistry.

Acknowledgements. This research was supported by the University of California at Berkeley, the University of California Agricultural Experiment Station, the U.S. Environmental Protection Agency (Cooperative Agreement CR-825610-01-0), and the University of California at Berkeley's Committee on Research. Much of the meteorological equipment and the measurement tower were loaned to us by the National Center for Atmospheric Research (NCAR). Also, for their invaluable assistance and patient counsel, we would like to thank Meredith Bauer, Jeanne Panek, Jean-Marc Fracheboud, Gunnar Schade, Ronald Cohen, T.N. Narasimhan, Alex Guenther, Brad Baker, Jim Greenberg, EPA Project Officer Christopher Geron, Bob Heald, and the Blodgett Forest crew.

References

Ackman, R. G., Fundamental groups in the response of flame ionization detectors to oxygenated aliphatic hydrocarbons, *J. Gas Chromatogr.*, *2*, 173-179, 1964.

Ackman, R. G., The flame ionization detector: further comments on molecular breakdown and fundamental group responses, *J. Gas Chromatogr.*, *6*, 497-501, 1968.

Andreae, M. O., and P. J. Crutzen, Atmospheric aerosols: Biogeochemical sources and role in atmospheric chemistry, *Science*, *276*, 1052-1058, 1997.

Apel, E. C., J. G. Calvert, J. P. Greenberg, D. Riemer, R. Zika, T. E. Kleindienst, W. A. Lonneman, K. Fung, and E. Fujita, Generation and validation of oxygenated volatile organic carbon standards for the 1995 Southern Oxidants Study Nashville Intensive, *J. Geophys. Res.*, *103*, 22,281- 22,294, 1998a.

Apel, E. C., J. G. Calvert, D. Riemer, W. Pos, R. Zika, T. E. Kleindienst, E. Fujita, K. Fung, W. A. Lonneman, P. B. Shepson, and T. K. Starn, Measurements comparison of oxygenated volatile organic compounds at a rural site during the 1995 SOS Study Nashville Intensive, *J. Geophys. Res.*, *103*, 22,295- 22,316, 1998b.

Aschmann, S. A., J. Arey, and R. Atkinson, OH radical formation from the gas-phase reactions of O_3 with methacrolein and methyl vinyl ketone, *Atmos. Environ.*, *30*, 2939-2943, 1996.

Atkinson, R., Kinetics and mechanisms of the gas-phase reactions of the hydroxyl radical with organic compounds, *J. Phys. Chem. Ref. Data Monogr.*, *1*, 1989.

Blades, A. T., The flame ionization detector, *J. Chromatogr. Sci.*, *11*, 251-255, 1973.

Buhr, M., et al., Evaluation of ozone precursor source types using principal component analysis of ambient air measurements in rural Alabama, *J. Geophys. Res.*, *100*, 22,853-22,860, 1995.

California Air Resources Board (CARB), California ambient air quality data 1980-1996, Tech. Support Div./Air Qual. Data Branch, Client Support Serv. Sect., Calif. Environ. Prot. Agency, Sacramento, 1997.

Chameides, W. L., R. W. Lindsay, J. Richardsen, and C.S. Kiang, The role of biogenic hydrocarbons in urban photochemical smog: Atlanta as a case study, *Science*, *241*, 1473-1475, 1988.

Christoffersen, T.S., J. Hjorth, O. Horie, N.R. Jensen, D. Kotzias, L.L. Molander, P. Neeb, L. Ruppert, R. Winterhalter, A. Virkkula, K. Wirtz, and B. R. Larsen, cis-pinic acid, a possible precursor for organic aerosol formation from ozonolysis of α-pinene, *Atmos. Environ.*, *32*, 1657-1661, 1998.

Derwent, R. G., Air chemistry and terrestrial gas emissions: A global perspective, *Philos. Trans. R. Soc. London, Ser. A*, *351*, 205-217, 1995.

Farmer, C.T., P. J. Milne, D.D. Riemer, and R.G. Zika, Continuous hourly analysis of C_2-C_{10} non-methane hydrocarbon compounds in urban air by GC-FID, *Environ. Sci. Technol.*, *28*, 238-245, 1994.

Goldan, P. D., W.C. Kuster, F.C. Fehsenfeld, and S.A. Montzka, The observation of a C_5 alcohol emission in a North American pine forest, *Geophys. Res. Lett.*, *20*, 1039-1042, 1993.

Goldan, P. D., W.C. Kuster, F.C. Fehsenfeld, and S.A. Montzka, Hydrocarbon measurements in the southeastern United States: The Rural Oxidants in the Southern Environment, *J. Geophys. Res.*, *100*, 25945-25963, 1995.

Goldan, P. D., W. C. Kuster, and F. C. Fehsenfeld, Nonmethane hydrocarbon measurements during the Tropospheric OH Photochemistry Experiment, *J. Geophys. Res.*, *102*, 6315-6324, 1997.

Goldstein, A. H., B.C. Daube, J.W. Munger, and S.C. Wofsy, Automated in-situ monitoring of atmospheric non-methane hydrocarbon concentrations and gradients, *J. Atmos. Chem.*, *21*, 43-59, 1995a.

Goldstein, A. H., C.M. Spivakovsky, and S. C. Wofsy, Seasonal variations of non-methane hydrocarbons in rural New England: Constraints on OH concentrations in northern midlatitudes, *J. Geophys. Res.*, *100*, 21,023-21,033, 1995b.

Goldstein, A. H., S.M. Fan, M.L. Goulden, J.W. Munger, and S.C. Wofsy, Emissions of ethene, propene and 1-butene by a midlatitude forest, *J. Geophys. Res.*, *101*, 9149-9157, 1996.

Goldstein, A. H. , M. L. Goulden, J. W. Munger, S. C. Wofsy, and C. D. Geron, Seasonal course of isoprene emissions from a midlatitude deciduous forest, *J. Geophys. Res.*, *103*, 31,045-31,056, 1998.

Greenberg, J. P., B. Lee, D. Helmig, and P. R. Zimerman, Fully automated gas chromatograph-flame ionization detector for the in situ determination of atmospheric non-methane hydrocarbons at low parts per trillion concentration, *J. Chromatogr.*, *676*, 389-398, 1994.

Harley, P., V. Fridd-Stroud, J. Greenberg, A. Guenther, and P. Vasconcellos, Emission of 2-methyl-3-buten-2-ol by pines: A potentially large source of reactive carbon to the atmosphere, *J. Geophys. Res., 103*, 25,479-25,486, 1998.

Hirsch, A. I., J.W. Munger, D.J. Jacob, L.W. Horowitz, and A.H. Goldstein, Seasonal variation of the ozone production efficiency per unit NO_x at Harvard Forest, Massachusetts, *J. Geophys. Res., 101*, 12,659-12,666, 1996.

Jorgensen, A. D., et al., Prediction of gas chromatography flame ionization detector response factors from molecular structures, *Anal. Chem., 62*, 683-689, 1990.

Lerdau, M., M. Litvak, P. Palmer, and R. Monson, Controls over monoterpene emissions from boreal forest conifers, *Tree Physiol., 17*, 563-569, 1997.

McKeen, S.A., and S. C. Liu, Hydrocarbon ratios and photochemical history of air masses, *Geophys. Res. Lett., 20*, 2363-2366, 1993.

McKeen, S.A., G. Mount, F. Eisele, E. Williams, J. Harder, P. Goldan, W. Kuster, S. C. Liu, K. Bauman, D. Tanner, A. Fried, S. Sewell, C. Cantrell, and R. Shetter, Photochemical modeling of hydroxyl and its relationship to other species during the Tropospheric OH Photochemistry Experiment, *J. Geophys. Res., 102*, 6467-6493, 1997.

Montzka, S. A., M. Trainer, W.M. Angevine, and F.C. Fehsenfeld, Measurements of 3-methyl furan, methyl vinyl ketone, and methacrolein at a rural forested site in the southeastern United States, *J. Geophys. Res., 100*, 11,393-11,401, 1995.

National Research Council (NRC), *Rethinking the Ozone Problem in Urban and Regional Air Pollution*, Nat. Acad. Press, Washington, D.C., 1991.

Parrish, D. D., et al., Indications of photochemical histories of Pacific air masses from measurements of atmospheric trace species at Point Arena, California, *J. Geophys. Res., 97*, 15,883-15,901, 1992.

Rudich, Y., R. Talukdar, J. B. Burkholder, and A. R. Ravishankara, Reaction of methylbutenol with hydroxyl radical: Mechanism and atmospheric implications, *J. Phys. Chem., 99*, 12,188-12,194, 1995.

Scanlon, J. T., Calculation of flame ionization detector relative response factors using the effective carbon number concept, *J. Chromatogr. Sci., 23*, 333-340, 1985.

Seinfeld, J. H., Urban air pollution: State of the science, *Science, 243*, 745-752, 1989.

Singh, H. B., et al., Acetone in the atmosphere: Distribution, sources, and sinks, *J. Geophys. Res., 99*, 1805-1819, 1994.

Singh, H. B., M. Kanakidou, P. J. Crutzen, and D. J. Jacobs, High concentrations and photochemical fate of oxygenated hydrocarbons in the global troposphere, *Nature, 78*, 50-54, 1995.

Sternberg, J. C., W. S. Galloway, and D. T. L. Jones, The mechanism of response of flame ionization detectors, in *Gas Chromatography*, edited by N. Brenner, J.E. Callen, and M. D. Weiss, Academic, San Diego, Calif., 1962.

Trainer, M., E. Y. Hsie, S. A. McKeen, R. Tallamraju, D. D. Parrish, F. C. Fehsenfeld, and S. C. Liu, Impact of natural hydrocarbons on hydroxyl and peroxy radicals at a remote site, *J. Geophys. Res., 92*, 11,879-11,894, 1987.

Williams, J., et al., Regional ozone from biogenic hydrocarbons deduced from airborne measurements of PAN, PPN, and MPAN, *Geophys. Res. Lett., 24*, 1099-1102, 1997.

Zhang, S., M. Shaw, J.H. Seinfeld, and R.C. Flagan, Photochemical aerosol formation from α-pinene and β-pinene, *J. Geophys. Res., 97*, 20,717-20,729, 1992.

A. H. Goldstein and M. S. Lamanna, University of California, Berkeley, 151 Hilgard Hall, Berkeley, CA 94720-3110. (e-mail: ahg@nature.berkeley.edu)

(Received November 2, 1998; revised April 9, 1999; accepted April 13, 1999.)